ACS OMEGA

http://pubs.acs.org/journal/acsodf

Article

Unraveling the Atomic Structures of 10-Electron (10e) Thiolate-Protected Gold Nanoclusters: Three $Au_{32}(SR)_{22}$ Isomers, One $Au_{28}(SR)_{18}$, and One $Au_{33}(SR)_{23}$

Pengye Liu, Wenhua Han, Mengke Zheng, Wenliang Li,* and Wen Wu Xu*

Cite This: *ACS Omega* 2021, 6, 10497−10503

Read Online

ACCESS | Metrics & More | Article Recommendations | Supporting Information

ABSTRACT: The atomic structures of 10-electron (10e) thiolate-protected gold nanoclusters have not received extensive attention both experimentally and theoretically. In this paper, five new atomic structures of 10e thiolate-protected gold nanoclusters, including three $Au_{32}(SR)_{22}$ isomers, one $Au_{28}(SR)_{18}$, and one $Au_{33}(SR)_{23}$, are theoretically predicted. Based on grand unified model (GUM), four Au_{17} cores with different morphologies can be obtained via three different packing modes of five tetrahedral Au_4 units. Then, five complete structures of three $Au_{32}(SR)_{22}$ isomers, one $Au_{28}(SR)_{18}$, and one $Au_{33}(SR)_{23}$ isomers can be formed by adding the thiolate ligands to three Au_{17} cores based on the interfacial interaction between thiolate ligands and gold core in known gold nanoclusters. Density functional theory calculations show that the relative energies of three newly predicted $Au_{32}(SR)_{22}$ isomers are quite close to two previously reported isomers. In addition, five new 10e gold nanoclusters have large highest occupied molecular orbital−lowest unoccupied molecular orbital (HOMO−LUMO) gaps and all-positive harmonic vibration frequencies, indicating their high stabilities.

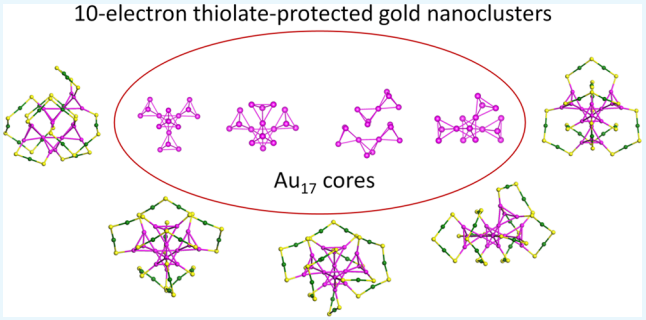

INTRODUCTION

Over the past years, the structures of thiolate-protected gold nanoclusters, expressed as $Au_m(SR)_n$, have facilitated abundant experimental and theoretical research efforts.[1−4] A large number of thiolate-protected gold nanoclusters with different free valence electron numbers have been obtained via both experimental X-ray crystallography and theoretical predictions, as shown in Table S1, in which the gold nanoclusters with different free valence electron numbers covering 4e, 6e, 8e, 10e, 12e, 14e, 16e, 18e, 20e, etc. were summarized. Among medium-sized clusters with different free valence electron numbers, there are many structures of 8e gold nanoclusters, i.e., $Au_{23}(SR)_{16}^-$, $Au_{24}(SR)_{16}$, $Au_{25}(SR)_{18}^-$, $Au_{28}(SR)_{20}$, etc.[5−11] Taking $Au_{28}(SR)_{20}$ nanoclusters as an example, two crystallized isomers and four predicted isomers were reported.[8−11] However, it shows that 10e thiolate-protected gold nanoclusters have not received extensive attention. No crystallized structures of 10e gold nanoclusters were experimentally determined and only three predicted structures, i.e., $Au_{29}(SR)_{19}$ and two $Au_{32}(SR)_{22}$ isomers, were theoretically proposed,[11,12] which hinders the deep understanding and controllable design of the 10e thiolate-protected gold nanoclusters.

With the development of theoretical models, i.e., "divide and protect" rule,[13] superatom complex (SAC) model,[14] superatom network (SAN) model,[15] grand unified model (GUM),[16,17] and so on, the model-guided design of the theoretical structures of thiolate-protected gold nanoclusters have become increasingly feasible. Taking GUM as an example, the structures of the gold cores in $Au_m(SR)_n$ can be viewed as several elementary blocks of triangular Au_3 and tetrahedral Au_4, obeying the dual rule packing or fusing together. As a consequence, based on GUM, the gold cores with different sizes and morphologies can be constructed via fusing or packing the elementary blocks. Then, the thiolate ligands can be added to the designed gold cores to form the complete structures of the thiolate-protected gold nanoclusters based on the interfacial interaction between thiolate ligands and gold core in known gold nanoclusters. Following this way, the full picture of one-dimensional (1D) and two-dimensional (2D) growth modes of $Au_{28+4n}(SR)_{20+2n}$ (n = 0−8) nanoclusters were presented based on GUM by predicting 15 theoretical structures of thiolate-protected gold nanoclusters.[10,11,18,19] Among them, the predicted $Au_{36}(SR)_{24}$ with 2D growth mode was confirmed by experimental X-ray crystallography.[19]

Received: March 12, 2021
Accepted: March 29, 2021
Published: April 9, 2021

In this work, five new 10e thiolate-protected gold nanoclusters including three $Au_{32}(SR)_{22}$ isomers, one $Au_{28}(SR)_{18}$, and one $Au_{33}(SR)_{23}$ are theoretically predicted based on GUM. Density functional theory (DFT) calculations show that these structures have large highest occupied molecular orbital−lowest unoccupied molecular orbital (HOMO−LUMO) gaps and all-positive vibrational frequencies, indicating their high stabilities.

CALCULATION METHODS

All of the predicted structures (−R group is replaced by −H) in this work were optimized using the DFT method implemented in the Gaussian 09 program package.[20] The Perdew−Burke−Ernzerhof (PBE) and Becke's three-parameter hybrid functional with the Lee−Yang−Parr correlation functional B3LYP,[21,22] all-electron basis set 6-31G* for H and S, and effective-core basis set LANL2DZ for Au were applied. Then, the time-dependent DFT was employed to calculate the absorption spectra of the thiolate-protected gold nanoclusters in this work.

RESULTS AND DISCUSSION

Up to date, only three 10e thiolate-protected gold nanoclusters, i.e., $Au_{29}(SR)_{19}$ and two $Au_{32}(SR)_{22}$ isomers, were theoretically proposed. $Au_{29}(SR)_{19}$ was obtained from

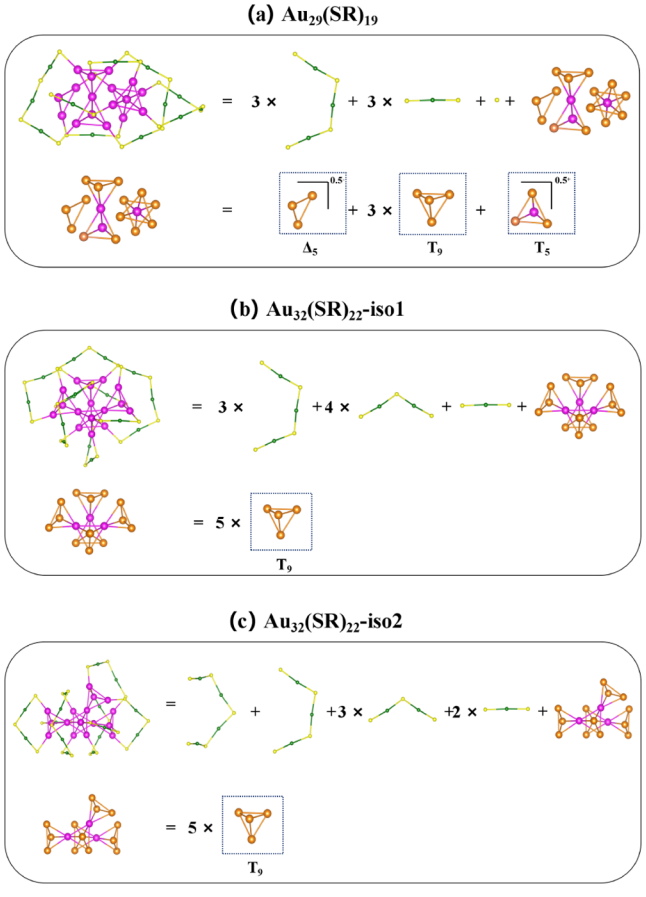

Figure 1. Structural decompositions of $Au_{29}(SR)_{19}$ (a), $Au_{32}(SR)_{22}$-Iso1 (b), and $Au_{32}(SR)_{22}$-Iso2 (c). Au atoms with 1e valence electrons are presented in wine and green. Au atoms with 0.5e valence electrons are presented in gold. S is presented in yellow. The R groups were omitted for clarity.

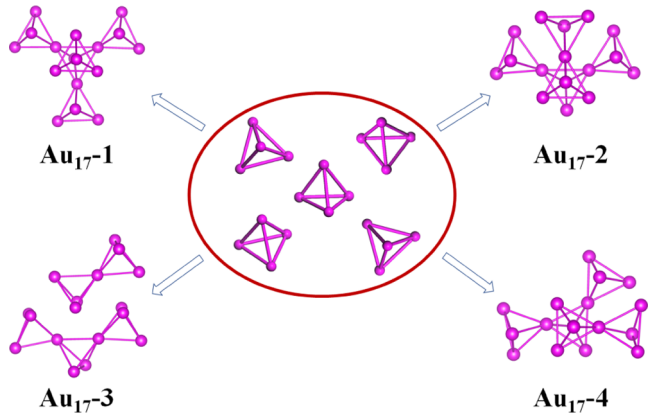

Figure 2. Different packing modes of five tetrahedral Au_4 elementary blocks resulting in four kinds of Au_{17} cores with different morphologies, i.e., Au_{17}-1, Au_{17}-2, Au_{17}-3, and Au_{17}-4.

Table 1. Computed Relative Energies, HOMO−LUMO Gaps, and the Lowest Vibrational Frequencies of Five $Au_{32}(SR)_{22}$ Isomers Using the PBE Functional[a]

	relative energy (eV)	HOMO−LUMO gaps (eV)	lowest vibrational frequency (cm^{-1})
$Au_{32}(SR)_{22}$-Iso1	0.00	1.74	6.59
$Au_{32}(SR)_{22}$-Iso2	0.39	1.58	6.63
$Au_{32}(SR)_{22}$-Iso3	0.51	1.55	10.51
$Au_{32}(SR)_{22}$-Iso4	0.55	1.74	5.06
$Au_{32}(SR)_{22}$-Iso5	0.55	1.90	6.75

[a]The R groups are simplified by H atoms.

$Au_{28}(SR)_{20}$ and $Au_{30}(SR)_{18}$ nanoclusters via the "gold-atom insertion, thiolate-group elimination" mechanism.[12] A new atomic structure of $Au_{32}(SR)_{22}$ (referred to as $Au_{32}(SR)_{22}$-Iso1) was predicted as an intermediate structure of crystallized $Au_{28}(SR)_{20}$ and $Au_{36}(SR)_{24}$ via theoretical modulation of the double-helical cores of experimentally determined nanoclusters.[11] In addition, the structure of the $Au_{32}(SR)_{22}$ isomer (referred to as $Au_{32}(SR)_{22}$-Iso2) was obtained based on GUM.[18] It can be found that the above three 10e thiolate-protected gold nanoclusters have the same number (17) of gold core atoms (Figure 1). The Au_{17} core of $Au_{29}(SR)_{19}$ can be viewed as four tetrahedral Au_4 and one triangular Au_3 elementary blocks packing or fusing together (Figure 1a). While both of the Au_{17} cores of two $Au_{32}(SR)_{22}$ isomers can be viewed as five tetrahedral Au_4 elementary blocks packing or fusing together (Figure 1b,c), indicating that the different packing modes of the same number (5) of elementary blocks can result in Au_{17} cores with different morphology.[10]

Actually, according to GUM,[16,17] different packing modes of five tetrahedral Au_4 elementary blocks can generate various cores. Here, four kinds of Au_{17} cores with different morphology, i.e., Au_{17}-1, Au_{17}-2, Au_{17}-3, and Au_{17}-4, are presented (Figure 2). Among them, Au_{17}-2 and Au_{17}-4 are the cores of two $Au_{32}(SR)_{22}$ isomers ($Au_{32}(SR)_{22}$-Iso1 and $Au_{32}(SR)_{22}$-Iso2).[11,18] Therefore, new atomic structures of 10e thiolate-protected gold nanoclusters can be predicted by adding the thiolate ligands on the designed Au_{17} cores based on the interfacial interaction between thiolate ligands and gold core in known gold nanoclusters.

For the Au_{17}-1 core, it can be viewed as removing three Au_4 units from the Au_{26} core of $Au_{44}(SR)_{28}$ following 2D growth

https://doi.org/10.1021/acsomega.1c01345
ACS Omega 2021, 6, 10497−10503

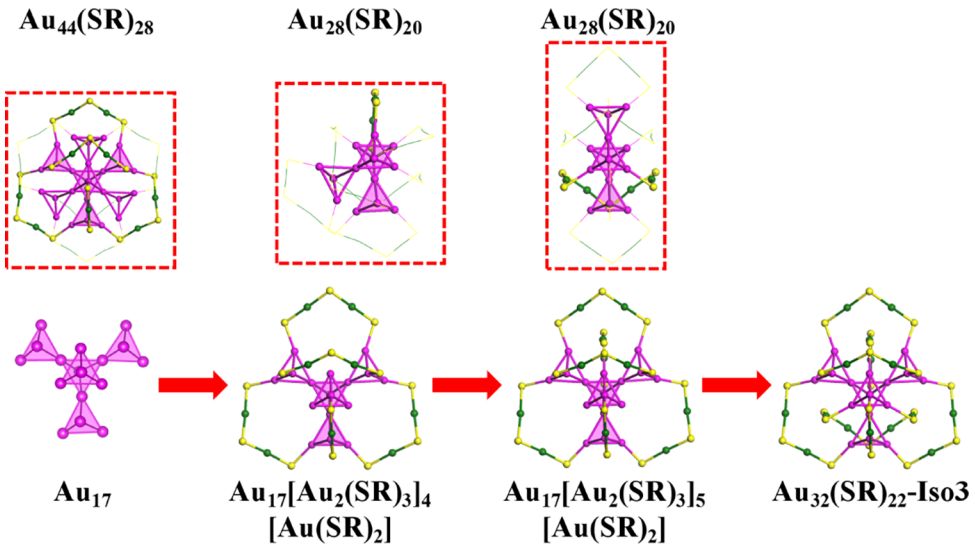

Figure 3. Structural prediction of $Au_{32}(SR)_{22}$-Iso3. Au atoms are presented in wine, blue, and dark green, respectively. S is presented in yellow. The R groups are omitted for clarity.

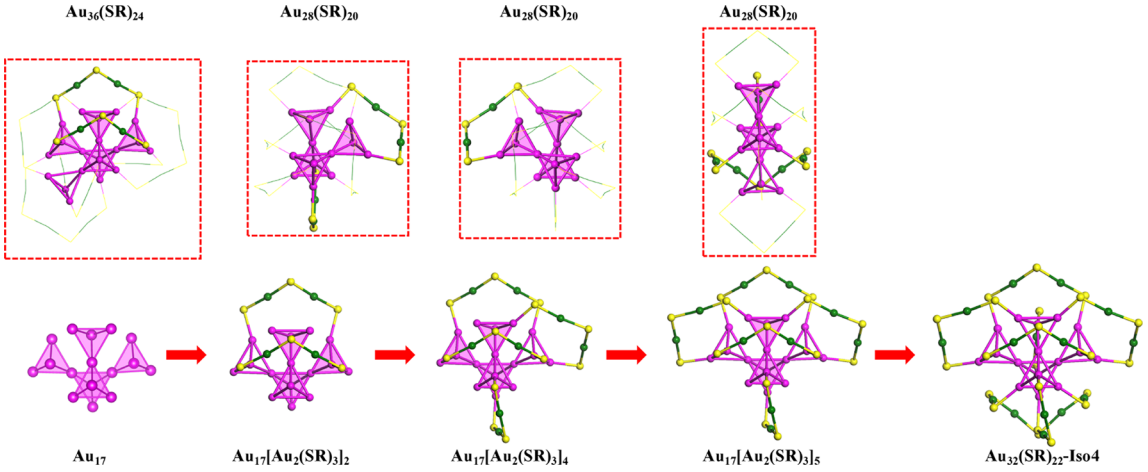

Figure 4. Structural prediction of $Au_{32}(SR)_{22}$-Iso4. Au atoms are presented in wine, blue, and dark green, respectively. S is presented in yellow. The R groups are omitted for clarity.

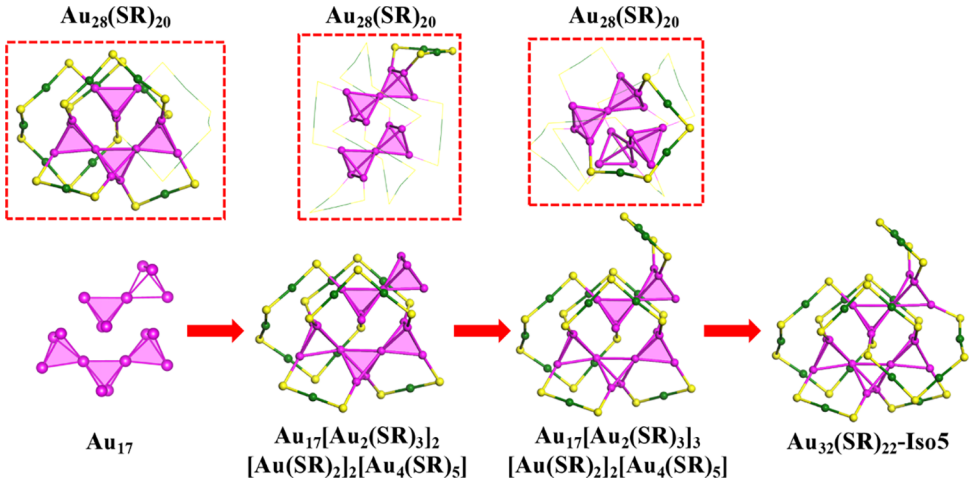

Figure 5. Structural prediction of $Au_{32}(SR)_{22}$-Iso5. Au atoms are presented in wine, blue, and dark green, respectively. S is presented in yellow. The R groups are omitted for clarity.

mode (Figure S1).[19] Since the Au_{17}-1 core (highlighted by filling with wine color in Figure 3) can be found in the Au_{26} core of $Au_{44}(SR)_{28}$, four $[Au_2(SR)_3]$ and one $[Au(SR)_2]$ can be combined with the Au_{17}-1 core come to form the

https://doi.org/10.1021/acsomega.1c01345
ACS Omega 2021, 6, 10497−10503

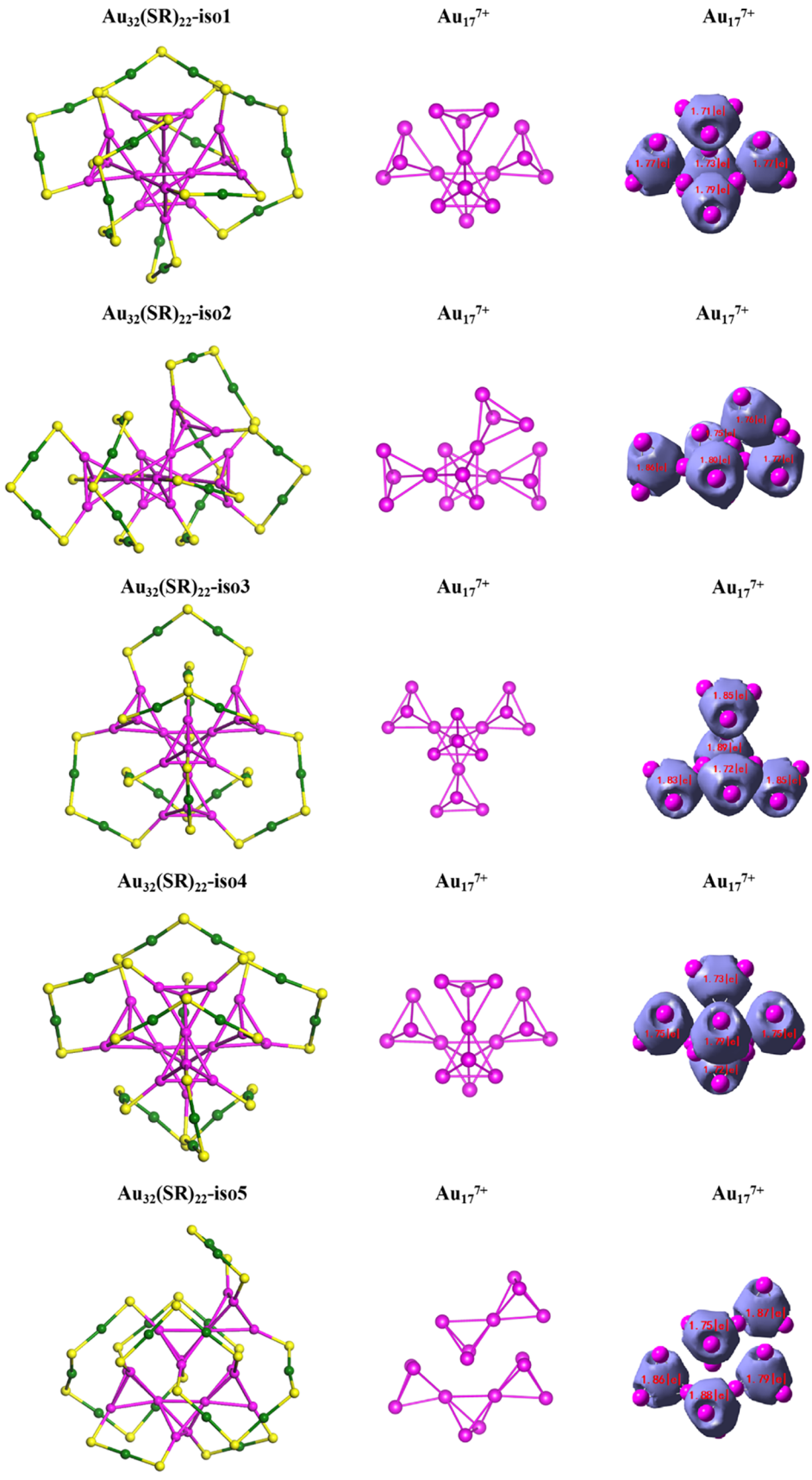

Figure 6. Structures of five $Au_{32}(SR)_{22}$ isomers as well as their Au_{17}^{7+} cores and the visualization of the valence electron distributions in the Au_{17}^{7+} cores. Au atoms are presented in wine, blue, and dark green, respectively. S is presented in yellow.

https://doi.org/10.1021/acsomega.1c01345
ACS Omega 2021, 6, 10497−10503

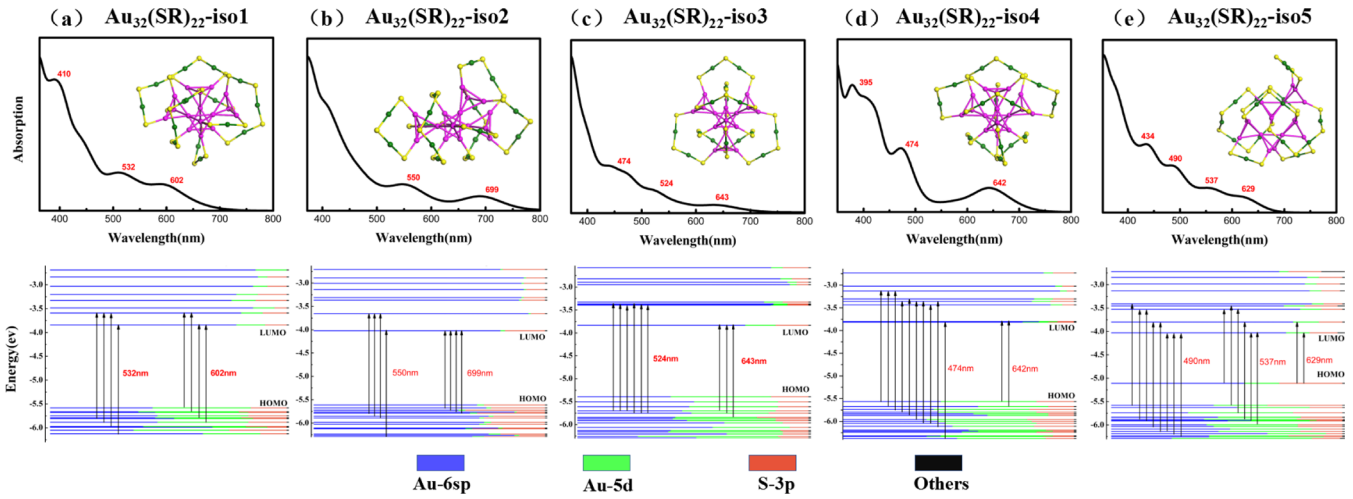

Figure 7. Computed absorption spectra and diagrams of the Kohn−Sham (KS) orbital energy levels of five $Au_{32}(SR)_{22}$ isomers. The prominent absorption peaks are highlighted in red. The R groups are simplified by H atoms.

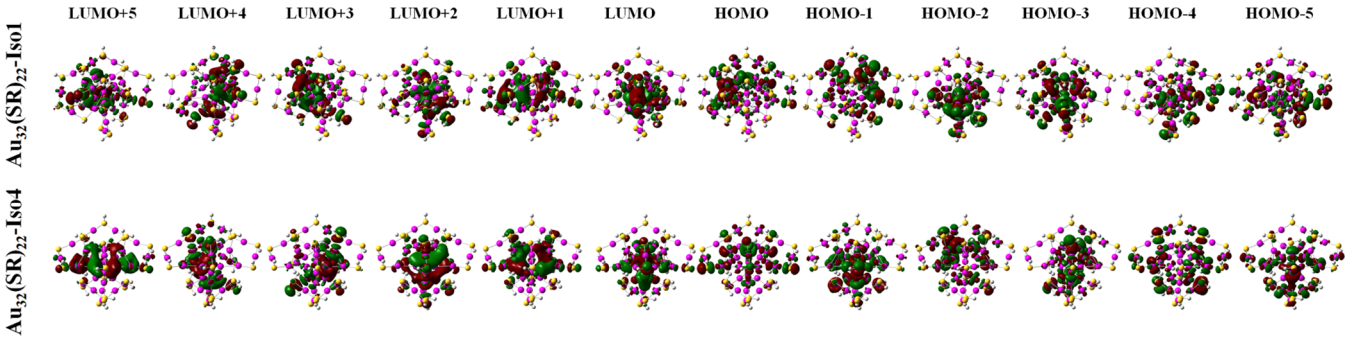

Figure 8. Molecular orbitals from HOMO − 5 to LUMO + 5 for $Au_{32}(SR)_{22}$-Iso1 (upper panel) and $Au_{32}(SR)_{22}$-Iso4 (lower panel).

Table 2. Orbital Contributions from HOMO − 5 to LUMO + 5

	Au(6sp)		Au(5d)		S(3p)	
	$Au_{32}(SR)_{22}$-Iso1 (%)	$Au_{32}(SR)_{22}$-Iso4 (%)	$Au_{32}(SR)_{22}$-Iso1 (%)	$Au_{32}(SR)_{22}$-Iso4 (%)	$Au_{32}(SR)_{22}$-Iso1 (%)	$Au_{32}(SR)_{22}$-Iso4 (%)
LUMO + 5	84.69	93.49	6.38	2.97	8.17	3.21
LUMO + 4	78.23	81.62	9.33	8.29	11.87	9.60
LUMO + 3	75.89	80.91	10.48	8.34	13.08	10.41
LUMO + 2	85.04	88.68	6.37	4.95	8.26	6.04
LUMO + 1	79.81	84.15	9.58	7.40	10.32	8.18
LUMO	75.92	76.89	11.71	10.86	11.92	11.94
HOMO	42.76	42.19	41.45	41.19	15.61	16.50
HOMO − 1	36.79	57.78	42.57	30.22	20.47	11.85
HOMO − 2	44.10	38.99	38.88	41.18	16.89	19.69
HOMO − 3	45.15	41.22	37.90	41.80	16.76	16.83
HOMO − 4	44.04	55.61	36.46	32.33	19.38	11.99
HOMO − 5	52.44	61.98	33.41	25.53	14.01	12.37

$Au_{17}[Au_2(SR)_3]_4[Au(SR)_2]$ structure. Similarly, since the Au_{17}-1 core has the same Au_{14} structure (highlighted by filling with wine color in Figure 3) as two $Au_{28}(SR)_{20}$ isomers do,[11,18] the $Au_{17}[Au_2(SR)_3]_4[Au(SR)_2]$ structure can further bind with one $[Au_2(SR)_3]$ and one $[Au_4(SR)_5]$ to form the complete structure of $Au_{32}(SR)_{22}$ (referred as $Au_{32}(SR)_{22}$-Iso3). The result shows that the protection motifs of $Au_{32}(SR)_{22}$-Iso3 are able to from $Au_{44}(SR)_{28}$ and two $Au_{28}(SR)_{20}$ structures.

For the Au_{17}-2 core, it can be viewed as fusing one Au_4 on the Au_{14} core of $Au_{28}(SR)_{20}$ by sharing one gold atom or removing one tetrahedral Au_4 from the Au_{20} core of $Au_{36}(SR)_{24}$ (Figure S1).[11] Since the Au_{17}-2 core (highlighted by filling with wine color in Figure 4) can be found in the Au_{20} core of $Au_{36}(SR)_{24}$, two $[Au_2(SR)_3]$ can be combined with the Au_{17}-2 core to form the $Au_{17}[Au_2(SR)_3]_2$ structure, which can further bind with two $[Au_2(SR)_3]$ and one $[Au_4(SR)_5]$ to form the complete structure of $Au_{32}(SR)_{22}$ (referred as $Au_{32}(SR)_{22}$-Iso4) following the same way. The result shows that the protection motifs of $Au_{32}(SR)_{22}$-Iso4 can be obtained from $Au_{36}(SR)_{24}$ and two $Au_{28}(SR)_{20}$ structures. In addition, another new atomic structure of $Au_{28}(SR)_{18}$ can also be predicted by adding four $[Au_2(SR)_3]$ and three $[Au(SR)_2]$ on the Au_{17}-2 core, as shown in Figure S2. Therefore, it can be found that three predicted atomic structures, i.e., $Au_{32}(SR)_{22}$-

https://doi.org/10.1021/acsomega.1c01345
ACS Omega 2021, 6, 10497−10503

Iso1, $Au_{32}(SR)_{22}$-Iso4, and $Au_{28}(SR)_{18}$, have the same Au_{17}-2 core, suggesting that the structural predictions of these gold nanoclusters were achieved by redistributing the Au−S "staple" motifs on the same Au_{17}-2 core.[23]

For the Au_{17}-3 core, it can be viewed as fusing one Au_4 on the Au_{14} core of $Au_{28}(SR)_{20}$ by sharing one gold atom (Figure S1).[11] Similarly, the protection motifs on the Au_{17}-3 core can be obtained from three $Au_{28}(SR)_{20}$ isomers, resulting in the structural prediction of $Au_{32}(SR)_{22}$ (referred to as $Au_{32}(SR)_{22}$-Iso5) following the same way (Figure 5). In addition, another new atomic structure of $Au_{33}(SR)_{23}$ can also be predicted by adding two $[Au(SR)_2]$, two $[Au_2(SR)_3]$, four $[Au_3(SR)_4]$, and one $[Au_4(SR)_5]$ on the Au_{17}-3 core, as shown in Figure S3.

With the newly obtained structures of five 10e thiolate-protected gold nanoclusters, i.e., $Au_{32}(SR)_{22}$-Iso3, $Au_{32}(SR)_{22}$-Iso4, $Au_{32}(SR)_{22}$-Iso5, $Au_{28}(SR)_{18}$, and $Au_{33}(SR)_{23}$, and the previously predicted two 10e gold nanoclusters $Au_{32}(SR)_{22}$-Iso1 and $Au_{32}(SR)_{22}$-Iso2, the electronic properties of these nanoclusters was obtained by density functional theory (DFT) calculations using the PBE functional. As shown in Table 1, the computed relative energies of three newly predicted $Au_{32}(SR)_{22}$ isomers, i.e., $Au_{32}(SR)_{22}$-Iso3, $Au_{32}(SR)_{22}$-Iso4, and $Au_{32}(SR)_{22}$-Iso5, are close to that of two previously predicted isomers, i.e., $Au_{32}(SR)_{22}$-Iso1 and $Au_{32}(SR)_{22}$-Iso2. In addition, these five $Au_{32}(SR)_{22}$ isomers have large HOMO−LUMO gaps and all-positive harmonic vibrational frequencies, suggesting the likelihood of high chemical stabilities of the three predicted $Au_{32}(SR)_{22}$ isomers. For another two newly predicted 10e gold nanoclusters, i.e., $Au_{28}(SR)_{18}$ and $Au_{33}(SR)_{23}$, DFT calculations also show that both of them have large HOMO−LUMO gaps and all-positive harmonic vibrational frequencies (Table S2). The B3LYP functional was also used to check the relative energies of five $Au_{32}(SR)_{22}$ isomers (Table S3), showing they have very close relative energies. In addition, the superatom network model using the adaptive natural density partitioning analysis was used to describe the 10e thiolate-protected gold nanoclusters,[15,24] as shown in Figures 6 and S4. Taking the Au_{17}^{7+} cores of five $Au_{32}(SR)_{22}$ isomers as examples, we show that the 10e valence electrons of each $Au_{32}(SR)_{22}$ isomer are equally distributed on five tetrahedral Au_4 units. Thus, the Au_{17}^{7+} cores of each $Au_{32}(SR)_{22}$ isomer can be viewed as a network of five 4c−2e (4c denotes 4 centers). Similar behavior can also be seen in the Au_{17}^{7+} cores of $Au_{28}(SR)_{18}$ and $Au_{33}(SR)_{23}$ (Figure S4).

In Figures 7 and S5, the computed optical absorption spectra of 10e thiolate-protected gold nanoclusters are presented. Figure 7 shows that five $Au_{32}(SR)_{22}$ isomers have distinct absorption peaks. $Au_{32}(SR)_{22}$-Iso1 shows one step peak at 410 nm and two broad peaks at 532 and 602 nm, $Au_{32}(SR)_{22}$-Iso2 shows two broad peaks at 550 and 699 nm, $Au_{32}(SR)_{22}$-Iso3 shows three broad peaks at 474, 524 and 643 nm, $Au_{32}(SR)_{22}$-Iso4 shows three absorption peaks at 395, 474, and 642 nm, and $Au_{32}(SR)_{22}$-Iso5 shows two step peaks at 434 and 490 nm and two broad peaks at 537 and 629 nm. The distinct absorption peaks of five $Au_{32}(SR)_{22}$ isomers suggest they are all distinct isomers. In addition, the Kohn−Sham (KS) orbital energy levels of each 10e nanoclusters are also presented (Figures 7 and S5). Taking $Au_{32}(SR)_{22}$-Iso3 as an example, the absorption peak at 524 nm mainly stems from the HOMO + 3 to LUMO + 1, LUMO + 2 and LUMO + 3 and HOMO + 4 to LUMO + 1, LUMO + 2 and LUMO + 3, and the absorption peak at 643 nm mainly stems from HOMO + 3, HOMO + 4, and HOMO + 5 to LUMO. In addition, the absorption peaks of all of the $Au_{32}(SR)_{22}$ isomers mainly involve the Au(sp) → Au(sp) transitions.

In addition, due to the same Au_{17} core but different protection ligands between $Au_{32}(SR)_{22}$-Iso1 and $Au_{32}(SR)_{22}$-Iso4, the molecular orbitals from HOMO − 5 to LUMO + 5 as well as their contributions for both nanoclusters are presented in Figure 8 and Table 2, respectively. Although they have the same Au_{17} cores, it can be seen in Figure 8 that both $Au_{32}(SR)_{22}$-Iso1 and $Au_{32}(SR)_{22}$-Iso4 have different molecular orbitals, which can be attributed to the different protection ligands for both nanoclusters. This behavior is also reflected in their different orbital contributions in Table 2.

CONCLUSIONS

In summary, based on GUM and the interfacial interaction between thiolate ligands and gold core in known gold nanoclusters, the atomic structures of five 10e thiolate-protected gold nanoclusters are theoretically predicted. DFT calculations suggest these predicted 10e nanoclusters exhibit high chemical stabilities. We expect that the predictions of these structures could stimulate future experimental and theoretical interests in 10e thiolate-protected gold nanoclusters.

ASSOCIATED CONTENT

Supporting Information

The Supporting Information is available free of charge at https://pubs.acs.org/doi/10.1021/acsomega.1c01345.

Formation of Au_{17} cores, the structural predictions of $Au_{28}(SR)_{18}$ and $Au_{33}(SR)_{23}$, the visualization of the valence electron distributions in the Au_{17}^{7+} cores of $Au_{28}(SR)_{18}$ and $Au_{33}(SR)_{23}$, and the computed absorption spectra and diagrams of Kohn−Sham (KS) orbital energy levels of $Au_{28}(SR)_{18}$ and $Au_{33}(SR)_{23}$ (PDF)

AUTHOR INFORMATION

Corresponding Authors

Wenliang Li − *College of Energy Engineering, Xinjiang Institute of Engineering, Urumqi 830023, China*; Email: wenliangli@vip.126.com

Wen Wu Xu − *Department of Physics, School of Physical Science and Technology, Ningbo University, Ningbo 315211, China*; orcid.org/0000-0002-0651-9562; Email: xuwenwu@nbu.edu.cn

Authors

Pengye Liu − *Department of Physics, School of Physical Science and Technology, Ningbo University, Ningbo 315211, China*

Wenhua Han − *Department of Physics, School of Physical Science and Technology, Ningbo University, Ningbo 315211, China*

Mengke Zheng − *Department of Physics, School of Physical Science and Technology, Ningbo University, Ningbo 315211, China*

Complete contact information is available at: https://pubs.acs.org/10.1021/acsomega.1c01345

Notes

The authors declare no competing financial interest.

■ ACKNOWLEDGMENTS

The authors are supported by the Natural Science Foundation of China (Grant No. 11974195) and the National Key Research and Development Program of China (Grant No. 2016YFE0120900). The authors acknowledge computational support from the National Supercomputing Center in Guangzhou (NSCC-GZ)

■ REFERENCES

(1) Jin, R.; Zeng, C.; Zhou, M.; Chen, Y. Atomically Precise Colloidal Metal Nanoclusters and Nanoparticles: Fundamentals and Opportunities. *Chem. Rev.* **2016**, *116*, 10346−10413.
(2) Pei, Y.; Zeng, X. C. Investigating the Structural Evolution of Thiolate Protected Gold Clusters from First-Principles. *Nanoscale* **2012**, *4*, 4054−4072.
(3) Häkkinen, H. The Gold-Sulfur Interface at the Nanoscale. *Nat. Chem.* **2012**, *4*, 443−455.
(4) Fernando, A.; Weerawardene, K. L. D. M.; Karimova, N. V.; Aikens, C. M. Quantum Mechanical Studies of Large Metal, Metal Oxide, and Metal Chalcogenide Nanoparticles and Clusters. *Chem. Rev.* **2015**, *115*, 6112−6216.
(5) Das, A.; Li, T.; Nobusada, K.; Zeng, C.; Rosi, N. L.; Jin, R. Nonsuperatomic $[Au_{23}(SC_6H_{11})_{16}]^-$ Nanocluster Featuring Bipyramidal Au_{15} Kernel and Trimeric $Au_3(SR)_4$ Motif. *J. Am. Chem. Soc.* **2013**, *135*, 18264−18267.
(6) Crasto, D.; Barcaro, G.; Stener, M.; Sementa, L.; Fortunelli, A.; Dass, A. $Au_{24}(Sadm)_{16}$ Nanomolecules: X-Ray Crystal Structure, Theoretical Analysis, Adaptability of Adamantane Ligands to Form $Au_{23}(Sadm)_{16}$ and $Au_{25}(Sadm)_{16}$, and its Relation to $Au_{25}(SR)_{18}$. *J. Am. Chem. Soc.* **2014**, *136*, 14933−14940.
(7) Akola, J.; Walter, M.; Whetten, R. L.; Häkkinen, H.; Grönbeck, H. On the Structure of Thiolate-Protected Au_{25}. *J. Am. Chem. Soc.* **2008**, *130*, 3756−3757.
(8) Zeng, C.; Li, T.; Das, A.; Rosi, N. L.; Jin, R. Chiral Structure of Thiolate-Protected 28-Gold-Atom Nanocluster Determined by X-Ray Crystallography. *J. Am. Chem. Soc.* **2013**, *135*, 10011−10013.
(9) Chen, Y.; Liu, C.; Tang, Q.; Zeng, C.; Higaki, T.; Das, A.; Jiang, D.; Rosi, N. L.; Jin, R. Isomerism in $Au_{28}(SR)_{20}$ Nanocluster and Stable Structures. *J. Am. Chem. Soc.* **2016**, *138*, 1482−1485.
(10) Xu, W. W.; Zeng, X. C.; Gao, Y. The Structural Isomerism in Gold Nanoclusters. *Nanoscale* **2018**, *10*, 9476−9483.
(11) Xu, W. W.; Duan, X.; Zeng, X. C. Modulation of the Double-Helical Cores: A New Strategy for Structural Predictions of Thiolate-Protected Gold Nanoclusters. *J. Phys. Chem. Lett.* **2020**, *11*, 536−540.
(12) Xiong, L.; Peng, B.; Ma, Z.; Wang, P.; Pei, Y. A Ten-Electron (10e) Thiolate-Protected $Au_{29}(SR)_{19}$ Cluster: Structure Prediction and a 'Gold-Atom Insertion, Thiolate-Group Elimination' Mechanism. *Nanoscale* **2017**, *9*, 2895−2902.
(13) Häkkinen, H.; Walter, M.; Gronbeck, H. Divide and Protect: Capping Gold Nanoclusters with Molecular Gold-Thiolate Rings. *J. Phys. Chem. B* **2006**, *110*, 9927−9931.
(14) Walter, M.; Akola, J.; Lopez-Acevedo, O.; Jadzinsky, P. D.; Calero, G.; Ackerson, C. J.; Whetten, R. L.; Gronbeck, H.; Häkkinen, H. A Unified View of Ligand-Protected Gold Clusters as Superatom Complexes. *Proc. Natl. Acad. Sci. U.S.A.* **2008**, *105*, 9157−9162.
(15) Cheng, L.; Yuan, Y.; Zhang, X.; Yang, J. Superatom Networks in Thiolate-Protected Gold Nanoparticles. *Angew. Chem., Int. Ed.* **2013**, *52*, 9035−9039.
(16) Xu, W. W.; Zhu, B.; Zeng, X. C.; Gao, Y. A Grand Unified Model for Liganded Gold Clusters. *Nat. Commun.* **2016**, *7*, No. 13574.
(17) Xu, W. W.; Zeng, X. C.; Gao, Y. Application of Electronic Counting Rules for Ligand-Protected Gold Nanoclusters. *Acc. Chem. Res.* **2018**, *51*, 2739−2747.
(18) Liu, P.; Han, W.; Zheng, M.; Xu, W. W. Two-Dimensional Growth Mode of Thiolate-Protected Gold Nanoclusters $Au_{28+4n}(SR)_{20+2n}$ (n = 0−8): Compared with their One-Dimensional Growth Mode. *Nanoscale* **2020**, *12*, 20677−20683.
(19) Liu, X.; Xu, W. W.; Huang, X.; Wang, E.; Cai, X.; Zhao, Y.; Li, J.; Xiao, M.; Zhang, C.; Gao, Y.; Ding, W.; Zhu, Y. De Novo Design of $Au_{36}(SR)_{24}$ Nanoclusters. *Nat. Commun.* **2020**, *11*, No. 3349.
(20) Frisch, M. J.; Trucks, G. W.; Schlegel, H. B.; Scuseria, G. E.; Robb, M. A.; Cheeseman, J. R.; Scalmani, G.; Barone, V.; Mennucci, B.; Petersson, G. A.; Nakatsuji, H.; Caricato, M.; Li, X.; Hratchian, H. P.; Izmaylov, A. F.; Bloino, J.; Zheng, G.; Sonnenberg, J. L.; Hada, M.; Ehara, M.; Toyota, K.; Fukuda, R.; Hasegawa, J.; Ishida, M.; Nakajima, T.; Honda, Y.; Kitao, O.; Nakai, H.; Vreven, T.; Montgomery, J. A., Jr; Peralta, J. E.; Ogliaro, F.; Bearpark, M.; Heyd, J. J.; Brothers, E.; Kudin, K. N.; Staroverov, V. N.; Kobayashi, R.; Normand, J.; Raghavachari, K.; Rendell, A.; Burant, J. C.; Iyengar, S. S.; Tomasi, J.; Cossi, M.; Rega, N.; Millam, J. M.; Klene, M.; Knox, J. E.; Cross, J. B.; Bakken, V.; Adamo, C.; Jaramillo, J.; Gomperts, R.; Stratmann, R. E.; Yazyev, O.; Austin, A. J.; Cammi, R.; Pomelli, C.; Ochterski, J. W.; Martin, R. L.; Morokuma, K.; Zakrzewski, V. G.; Voth, G. A.; Salvador, P.; Dannenberg, J. J.; Dapprich, S.; Daniels, A. D.; Farkas, O.; Foresman, J. B.; Ortiz, J. V.; Cioslowski, J.; Fox, D. J. *Gaussian 09*, revision D; Gaussian, Inc.: Wallingford, CT, 2010.
(21) Perdew, J. P.; Burke, K.; Ernzerhof, M. Generalized Gradient Approximation Made Simple. *Phys. Rev. Lett.* **1996**, *77*, 3865−3868.
(22) Lee, C.; Yang, W.; Parr, R. G. Development of the Colle-Salvetti correlation-energy formula into a functional of the electron density. *Phys. Rev. B* **1988**, *37*, 785−789.
(23) Xu, W. W.; Lin, D.; Fu, J.; Zhao, W.; Duan, X.; Zeng, X. C. Chiral $Au_{22}(SR)_{17}^-$: A New Ligand-Binding Strategy for Structural Prediction of Thiolate-Protected Gold Nanocluster. *Chem. Commun.* **2020**, *56*, 2995−2998.
(24) Zubarev, D. Y.; Boldyrev, A. I. Developing Paradigms of Chemical Bonding: Adaptive Natural Density Partitioning. *Phys. Chem. Chem. Phys.* **2008**, *10*, 5207−5217.

https://doi.org/10.1021/acsomega.1c01345
ACS Omega 2021, 6, 10497−10503